




Acceleration correction to the binary-encounter Bethe model for the electron-impact ionization of molecules

Yuan-Cheng Wang ^{1,2,3,*}, Giorgio Visentin ^{2,3,†}, Li Guang Jiao ^{2,3,4,‡} and Stephan Fritzsche ^{2,3,5}

¹College of Physical Science and Technology, Shenyang Normal University, Shenyang 110034, People's Republic of China

²Helmholtz-Institut Jena, D-07743 Jena, Germany

³GSI Helmholtzzentrum für Schwerionenforschung GmbH, D-64291 Darmstadt, Germany

⁴College of Physics, Jilin University, Changchun 130012, People's Republic of China

⁵Theoretisch-Physikalisches Institut, Friedrich-Schiller-Universität Jena, 07743 Jena, Germany



(Received 4 December 2023; accepted 16 January 2024; published 7 February 2024)

We propose a generalized binary-encounter Bethe model (GBEB) based on corrected acceleration energies to predict the electron-impact ionization cross sections of molecules. The acceleration energy of the incident electron is inversely proportional to the molecular effective charge felt by the ejected electron. The symmetry of molecular orbitals is analyzed to determine the core and valence effective charges. We tested the GBEB model on several organic, inorganic, and atmospheric molecules with increasing complexity. The calculated total ionization cross sections are in better agreement with the experimental data than the predictions from the original BEB model. Another major advantage of the present model rests upon the convenience that it does not need any *ad hoc* correction used in previous BEB models.

DOI: [10.1103/PhysRevA.109.022804](https://doi.org/10.1103/PhysRevA.109.022804)

I. INTRODUCTION

Comprehensive measurements of the electron-impact ionization cross sections for molecules have been carried out in the past decades since the electron-impact ionization process is one of the most important inelastic electron collision processes employed in modeling the plasma physics and chemistry [1]. In the early years, experimental measurements were concentrated only on the total ionization cross sections [2–4]. Later, the measurement of partial ionization cross sections also attracted increasing interest [5–14]. The discrepancies between different measurements were found rather large for a few molecules (e.g., CS₂ [15–18]). Until recently, the theoretical estimation of the total ionization cross section was still one of the most important and challenging tasks in the study of electron-impact ionization of molecules. Furthermore, the total ionization cross sections can also be used to estimate the partial ionization cross sections for different molecular dissociative ionization channels [19].

Ab initio methods (e.g., the convergent close-coupling method [20,21], *R*-matrix method [22], and Schwinger variational principle theory [23]) have been proven to be very successful in the study of electron-molecule scattering processes, such as the elastic scattering and excitation [21]. For the electron-impact ionization process, due to the complexity of modeling a system composed of two free electrons and a molecular ion in the exit channel, only some simple molecular systems can be solved by these advanced many-electron methods. Therefore, for the general task of modeling the electron

impact ionization processes that involve complex molecules or the ionization of core molecular orbitals, the semi-empirical or semi-classical models stand in a proper position. These models are generally based on the additivity of contributions that arise from the individual molecular orbital to the total ionization cross section. In particular, the semi-empirical Deutsch-Märk model [24,25] and the binary-encounter Bethe (BEB) model [26,27] have been widely used to study the electron impact ionization of molecules. Recently, Falkowski *et al.* [28] proposed a model potential obtained by a fitting procedure using the BEB model cross sections, which could be used to account for the ionization channel in an electron-molecule collision calculation.

There have been a large number of studies on the electron-impact ionization of molecules by means of the well-known BEB model [27,29–33]. In this model, the Mott and Bethe approximations were combined to model the low- and high-energy collisions, respectively. The corresponding predictions are in reasonable agreement with the experimental data [2,5,27]. However, the predictive power and the applicability of this model are restricted by introducing *ad hoc* kinetic energy corrections for specific valence orbitals to reproduce the experimental data. For instance, Kim *et al.* [27,29,30] corrected the BEB model for several molecules containing atoms with $Z > 10$ by scaling the kinetic energies of the valence molecular orbitals using the highest principal quantum number of the atomic valence shell, i.e., $n = 3$. In a later work, Huo and Kim [33] provided two alternative corrections: (i) divide the potential energy of the chosen bound electron $\varepsilon_i + \langle p^2/2m \rangle$ by the principal quantum number ($n \geq 3$) of just those atomic orbitals that dominate the molecular orbital and (ii) calculate part of the valence electron kinetic energy by using the Hartree-Fock wave function with the effective core potential (ECP). Both of these two empirical corrections

*yuanchengwang@synu.edu.cn

†g.visentin@hi-jena.gsi.de

‡lgjiao@jlu.edu.cn

reduced the potential energy of the ejected electron and rescale the cross sections, but their applicability strongly depended on the experimental data. In this regard, Scott and Irikura [34,35] used both of these two corrections on a few molecules containing atoms with $Z > 10$, with correction (i) based upon all-electron (AE) Hartree-Fock calculations (BEB-AE), and (ii) with ECP-calculated energies (BEB-ECP). The scaling parameters included in both models were obtained by fitting the experimental cross sections.

During the last decade, organic molecules composed of C, H, O, and N atoms have been studied and the direct ionization cross sections have been calculated using the BEB model [36–42]. Recently, researchers have become increasingly interested in molecules containing atoms with $Z > 10$. The above-mentioned *ad hoc* corrections have also been used to calculate the electron impact ionization cross sections for fusion-relevant and organic molecules [19,43,44]. Nevertheless, for correction (i), not all energies of molecular orbitals containing atomic orbital with principal quantum number $n \geq 3$ are reduced. The Mulliken population should be evaluated, but the threshold of the Mulliken population is based on the comparison of the calculated ionization cross sections with the experimental data. For correction (ii), the contribution of core orbitals to the total ionization cross sections is missing due to the lack of core orbitals in the ECP calculations. The energies of core orbitals can be calculated by the AE Hartree-Fock method. However, the criteria for using either the ECP or AE approach are unclear. The BEB model alone does not tell explicitly which molecular orbitals should be preferably modeled by the AE energy-reduced or ECP-based calculations, representing a major drawback of the model. In these previous studies, the acceleration energy gained by the incident electron from the remaining electron and nucleus of the target is probably overestimated.

Recently, we revisited the BEB model for electron impact ionization of atoms [45]. The effective charge felt by the ejected electron turns out to play a remarkable role in the corresponding partial ionization cross sections. We derived a generalized form of “acceleration correction” for the kinetic energies of incident electron from Gauss’ law, which does not require any adjustable parameters or reduction corrections. The proposed generalized BEB (GBEB) gross ionization cross sections for the Xe atom, combined with the direct multiple ionizations by Montanari and Miraglia [46], agree very well with the experimental measurements in both the peak position and magnitude as well as in the high-energy behavior. The good agreement indicates that our GBEB model can probably be used to calculate the direct partial ionization cross sections of the outer shells of complex atoms. The original BEB model with a reduction of potential energies caused an overestimation of the peak value for the gross ionization cross sections of the Xe atom [47]. Similar results can be found for another noble gas atom, Ar. In the recent work by Fedus and Karwasz [48], these authors calculated the direct ionization cross sections by using the original BEB model without any reduction. For low incident energies, where excitation-autoionization contributes significantly, the BEB model cannot reproduce the sharp increase in the total ionization cross section observed in the experimental measurements [49]. However, the use of reduced potential

energies leads to a 20% overestimation of cross sections in the peak region, which is more serious than that in the Xe atom. The use of generalized “acceleration correction” based on effective charge is expected to provide reasonable direct partial ionization cross sections. For molecular targets, the acceleration correction should also be important in the electron impact direct ionization cross sections.

The purpose of this article is to improve the molecular BEB model for electron impact direct ionization of molecules by incorporating a physically suggested acceleration correction. Some of the molecules we study here contain atoms with $Z > 10$ (e.g., SiH, SiF, SO₂, and CS₂). The symmetry of the molecular orbitals is also taken into account to derive the effective charge for each molecular orbital since molecular orbitals in the same symmetry may screen each other, e.g., the ejected electron from valence molecular orbitals with the same symmetries should have different effective charges.

The rest of the paper is organized as follows. In Sec. II, a brief introduction of the present model is outlined. The increase of incident electron energy for the ionization of molecular orbitals arising from the linear combination of atomic core orbitals as well as of atomic valence orbitals are analyzed. In Sec. III, the present model is applied to the total ionization cross sections of diatomic molecules (SiH and SiF), triatomic molecules (H₂O, SO₂, and CS₂), and polyatomic molecules (CH₄, C₂H₄, and C₂H₂) with increasing complexities to test the applicability. Conclusions are presented in Sec. IV.

II. THEORY

The BEB model developed by Kim *et al.* [26,47] provides a parameter-free and easy-to-use formula for the direct partial ionization cross section of atomic and molecular targets. This method depends on the binding energy ε_b and the kinetic energy $\langle p^2/2m \rangle$ of the target orbital for any given incident electron energy ε_i . Kim *et al.* [26] combined the Mott cross section with the dipole term of the Bethe cross section, which considerably enhanced the applicability and accuracy of the estimated cross section. The BEB formula was derived by assuming that the differential oscillator strength for the ionization of an atom was similar to that of the H atom. Such an assumption simplified the calculation of electron impact ionization cross sections.

The BEB cross section for an atomic electron in the $(nl)^q$ shell, where q refers to the occupation number and for the incident electron with an energy in the binding energy unit of $t = \varepsilon_i/\varepsilon_b$ is given by

$$\sigma_{\text{BEB}} = \frac{4\pi a_0^2 q}{(\varepsilon_b/R)^2(t+u+1)} \left[\frac{\ln t}{2} \left(1 - \frac{1}{t^2}\right) + 1 - \frac{1}{t} - \frac{\ln t}{t+1} \right], \quad (1)$$

where R is the Rydberg energy, a_0 is the Bohr radius, and $u = \langle p^2/2m \rangle/\varepsilon_b$.

In the present work, we improve the BEB model by incorporating a physically derived acceleration correction. This model adheres to Kim *et al.*'s [26,47] criterion of being parameter-free and, furthermore, makes it unnecessary to

select molecular orbitals where reduced energies need to be applied. The binary-encounter approximation assumes that, during the period of the interaction between the incident electron and the ejected electron, the remaining electrons and the nucleus play no role. Replacing the derived denominator t by the ‘‘Burgess denominator’’ $t + u + 1$ compensates for such an approximation. The energy $u + 1$ in the ‘‘Burgess denominator’’ is considered as the increase of the kinetic energy Δt , which is equal to the absolute value of the initial potential energy of the ejected electron. Such a potential energy can be approximately represented by one electron potential energy under a core with effective charge Z_{eff} determined by the nucleus and screening electrons. However, the simple correction $u + 1$ may overestimate the increase of the kinetic energy Δt for the incident electron. Actually, the rest of the atomic target apart from the ejected electron has a positive unit charge, which provides an attractive potential to accelerate the incident electron. According to Gauss’ law, the ratio between the variation of the kinetic energy Δt and the potential energy $u + 1$ is proportional to $1/Z_{\text{eff}}$, i.e.,

$$\Delta t = (u + 1)/Z_{\text{eff}}. \quad (2)$$

Although the original BEB model was very successful in calculating total ionization cross sections of simple atoms and molecules, as the complexity of molecular targets increases, the discrepancies between results of the original BEB calculations and experimental data become increasingly large. The present generalized ‘‘acceleration correction’’ has been proven to play an important role in the inner-shell electron ionization of atomic targets [45]. Molecules have more complex electronic structures than atoms, and therefore, it is necessary to define some rules for determining the effective charge felt by the ejected electron. As a matter of fact, the molecular orbitals of a specific target can be divided into two groups: (i) core orbitals and (ii) valence orbitals. The effective charge numbers are defined differently for each group.

(i) For molecular orbitals arising from the linear combination of atomic core orbitals, the inner orbital with higher binding energy screens the orbitals with lower binding energies. Degenerate molecular orbitals arising from the combination of inner-core atomic orbitals (e.g., $1s_A \pm 1s_B$) are assumed to be strongly localized and thus do not screen each other. These degenerate orbitals are assumed to have the same core effective charge number. Therefore, the core effective charge of the nucleus and screening electrons for the ejected electron in a given molecular orbital reads

$$Z_{\text{eff}}^C = \sum_N Z_N - \left(\sum_{m \in A} q_m - 1 \right), \quad (3)$$

where Z_N represents the atomic number of the N th atom in the molecule, q_m stands for the occupation number of each molecular orbital m . The notation A represents a collection of molecular orbitals expanding from the innermost orbital to the specific orbital from which the electron is ejected. To this effective charge number, the number 1 is subtracted to account for the ejection of one electron.

(ii) The molecular orbitals arising from the linear combination of valence atomic orbitals are considered as the outermost molecular orbitals. They are delocalized over the molecule

TABLE I. Binding energy ε_b (eV), kinetic energy $(p^2/2m)$ (eV), electron occupation number q , core effective charge numbers Z_{eff}^C , and valence effective charge numbers Z_{eff}^V for diatomic molecules SiH and SiF. The lowest binding energies of each molecule marked by an asterisk are experimental data [52].

Molecule	Molecular orbital	ε_b	$(p^2/2m)$	q	Z_{eff}^C	Z_{eff}^V
SiH	2σ	168.05	360.72	2	12	
	1π	116.18	330.97	4	6	
	3σ	115.27	332.52	2	6	
	4σ	17.23	31.00	2	4	
	5σ	10.31	28.15	2		1
	2π	7.89*	23.54	1		1
SiF	3σ	168.23	360.78	2	18	
	4σ	116.53	331.26	2	12	
	1π	115.82	332.46	4	12	
	5σ	43.41	104.61	2	10	
	6σ	18.37	79.61	2	4	
	2π	18.00	81.45	4	4	
	7σ	16.30	43.17	1		1
	3π	7.28*	29.07	2		1

and their mutual screening is affected by their symmetries which affect their spatial distribution (e.g., σ_g and π_u molecular orbitals have different spatial distributions). Since the effective charge number is the sum over all nuclear charges minus the number of screening electrons, the effective charge for the valence molecular orbital with a given symmetry irreducible representation $r_{n,\pi}$ (rotoreflection symmetry r_n and parity π) can also be determined by the number of screened valence electrons of the same symmetry for neutral molecules. Thus, the valence orbital effective charge number is given by

$$Z_{\text{eff}}^V = 1 + \sum_{l \in B} q_l^{r_{n,\pi}}, \quad (4)$$

$q_l^{r_{n,\pi}}$ indicates the occupation number of the l th outer molecular orbitals, represented as collection B , with the same symmetry as the orbital out of which the electron is ejected. Typically, $Z_{\text{eff}}^V = 1$ is employed for almost all molecular valence orbitals considered in this work. However, for SO_2 , the effective charges for $7a_1$ valence orbital is 3 due to the existence of an outer $8a_1$ molecular orbital with an occupation number of 2. The same situation applies to the $4b_1$ valence orbital (due to the existence of an outer $5b_1$ orbital).

With this modification, the present GBEB electron impact partial ionization cross section of an atomic electron in the molecular orbital with binding energy ε_b is given by

$$\sigma_{\text{GBEB}} = \frac{4\pi a_0^2 q}{(\varepsilon_b/R)^2 (t + \Delta t)} \left[\frac{\ln t}{2} \left(1 - \frac{1}{t^2} \right) + 1 - \frac{1}{t} - \frac{\ln t}{t + 1} \right], \quad (5)$$

where Δt is given by Eq. (2).

We present the binding energy, kinetic energy, electron occupation number, core effective charge number, and valence effective charge number for diatomic molecules (SiH and SiF) in Table I, triatomic molecules (H_2O , SO_2 , and CS_2) in Table II, and polyatomic molecules (CH_4 , C_2H_4 ,

TABLE II. Binding energy ε_b (eV), kinetic energy $\langle p^2/2m \rangle$ (eV), electron occupation number q , core effective charge numbers Z_{eff}^C , and valence effective charge numbers Z_{eff}^V for triatomic molecules (H_2O , SO_2 , and CS_2). The lowest binding energies of each molecule marked by an asterisk are experimental data [52].

Molecule	Molecular orbital	ε_b	$\langle p^2/2m \rangle$	q	Z_{eff}^C	Z_{eff}^V
H_2O	$2a_1$	36.81	71.18	2	7	
	$1b_2$	19.44	48.69	2		1
	$3a_1$	15.92	58.45	2		1
	$1b_1$	12.61*	60.77	2		1
SO_2	$1b_1$	562.02	794.78	2	27	
	$2a_1$	562.02	794.78	2	27	
	$3a_1$	251.26	509.83	2	25	
	$2b_1$	187.65	478.79	2	23	
	$1b_2$	186.34	478.96	2	19	
	$4a_1$	186.31	479.56	2	19	
	$5a_1$	38.87	72.21	2	17	
	$3b_1$	36.50	78.45	2	15	
	$6a_1$	24.70	81.06	2	13	
	$7a_1$	18.18	68.50	2		3
	$4b_1$	17.91	57.17	2		3
	$2b_2$	16.80	50.69	2		1
	$5b_1$	14.26	65.20	2		1
	$1a_2$	13.77	64.28	2		1
CS_2	$8a_1$	12.50*	57.36	2		1
	$2\sigma_g$	310.70	436.27	2	33	
	$2\sigma_u$	246.20	509.11	2	29	
	$3\sigma_g$	246.20	509.13	2	29	
	$3\sigma_u$	182.59	478.09	2	25	
	$4\pi_g$	182.59	478.10	2	25	
	$1\pi_g$	181.29	478.88	4	17	
	$1\pi_u$	181.29	478.88	4	17	
	$5\sigma_g$	30.38	54.89	2	15	
	$4\sigma_u$	27.60	62.25	2	13	
	$6\sigma_g$	18.68	62.69	2	11	
	$5\sigma_u$	15.80	56.70	2		1
	$2\pi_u$	14.04	37.66	4		1
	$2\pi_g$	10.07*	47.64	4		1

and C_2H_2) in Table III. The kinetic and binding energies of molecular orbital were computed at the Hartree-Fock level with the aug-cc-pvTz basis set for all the atoms. The molecular orbital kinetic energies were computed with the PYSCF quantum chemistry software [50], while the molecular orbital binding energies were computed with the DIRAC23 [51] quantum chemistry software using a nonrelativistic Hamiltonian for consistency with the kinetic energy computation. In both sets of calculations the convergence energy threshold for the Hartree-Fock total energy was set to $10^{-10} E_h$. Due to the intrinsic limitations of the Hartree-Fock theory in modeling of valence electron correlation effects, we use the experimental ionization potentials for the lowest binding energies.

III. RESULTS AND DISCUSSIONS

A. Diatomic molecules

Figure 1 compares the present GBEB (aug-cc-pvTz) calculated ionization cross sections of the diatomic molecules

TABLE III. Binding energy ε_b (eV), kinetic energy $\langle p^2/2m \rangle$ (eV), electron occupation number q , core effective charge numbers Z_{eff}^C , and valence effective charge numbers Z_{eff}^V for polyatomic molecules (CH_4 , C_2H_4 , and C_2H_2). The lowest binding energies of each molecule marked by an asterisk are experimental data [52].

Molecule	Molecular orbital	ε_b	$\langle p^2/2m \rangle$	q	Z_{eff}^C	Z_{eff}^V
CH_4	$1a_1$	305.03	435.83	2	9	
	$2a_1$	25.66	33.02	2	7	
	$1t_2$	14.80*	25.93	6		1
C_2H_4	$2a_g$	28.02	40.36	2	9	
	$2b_{2u}$	21.45	33.53	2	9	
	$1b_{3u}$	17.47	25.18	2		1
	$3a_g$	15.93	34.73	2		1
	$1b_{1g}$	13.78	28.45	2		1
C_2H_2	$1b_{1u}$	10.51*	25.82	2		1
	$1\sigma_g$	306.04	435.22	2	11	
	$1\sigma_u$	305.93	436.35	2	11	
	$2\sigma_g$	28.07	48.53	2	9	
	$2\sigma_u$	20.84	32.79	2	7	
	$3\sigma_g$	18.51	33.37	2		1
	$1\pi_u$	11.40*	28.53	4		1

SiH and SiF with the BEB ($u/3$) results by Ali *et al.* [30] and Hwang *et al.* [27]. The notation “ $u/3$ ” means the kinetic energies of the valence molecular orbitals were scaled by the highest atomic valence principal quantum number $n = 3$. To show the limitations of the BEB model, we also present the unscaled BEB reference data and our GBEB cross sections with the molecular orbital kinetic and binding energies in Refs. [27,30]. These energies were computed at the Hartree-Fock level with the 6-311G basis set. We labeled these calculations as BEB (6-311G) and GBEB (6-311G), respectively. In Fig. 1, we also compare the present results with the existing experimental data by Hayes *et al.* [7] and Tarnovsky *et al.* [10].

For the SiH molecule shown in Fig. 1(a), the GBEB (aug-cc-pvTz) and the GBEB (6-311G) predictions are in good agreement with the measurements by Tarnovsky *et al.* [10] in the low incident energy region, while the BEB ($u/3$) results slightly overestimate the experimental data. The BEB (6-311G) results underestimate the experimental data, and this deviation increases as the incident energy approaches the peak position. All theoretical predictions underestimate the experimental data at incident energies greater than 80 eV. This is probably due to the absence of multiple ionization contributions, such as the ionization followed by the dissociative autoionization. For the SiF molecule shown in Fig. 1(b), the GBEB (aug-cc-pvTz) and the GBEB (6-311G) predictions are in better agreement with the experimental data by Hayes *et al.* [7] than the BEB ($u/3$) results for incident energies above 50 eV. In this high-incident energy region, all theoretical results are within the error bars, except that the BEB (6-311G) predictions underestimate the experimental data. It is worth mentioning that small portions of Si Rydberg atoms were produced in the experimental measurements by Hayes *et al.* [7]. Due to the very large electron impact ionization cross sections of these species, the Si^+ signals detected from Rydberg atom ionization in the electron beam were

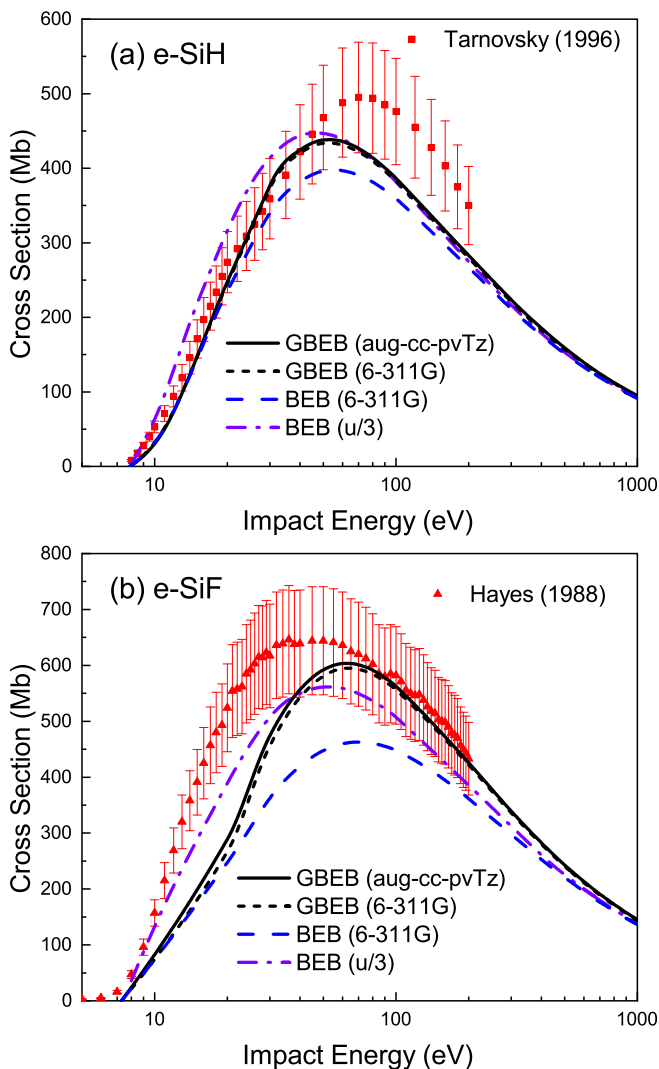


FIG. 1. Total ionization cross sections for diatomic molecules (a) SiH and (b) SiF. The results of the present GBEB cross sections are shown and compared with the BEB calculations, black solid line: GBEB (aug-cc-pvTz); black short dashed line: GBEB (6-311G); blue dashed line: BEB (6-311G) [27,29,30]; purple dashed dotted line: BEB ($u/3$) [27,29,30]. Comparison of the theoretical results with the experimental data are also shown, red triangles: Hayes *et al.* [7]; red squares: Tarnovsky *et al.* [10].

comparable to the Si^+ signal detected from dissociative ionization of SiF. This process may lead to an increase of the measured electron impact ionization cross sections at low incidence energy.

The comparison among the theoretical results in Fig. 1 shows large amount of similarities in these two molecules. Our GBEB (aug-cc-pvTz) and the GBEB (6-311G) predictions are close to each other, which indicates that both the aug-cc-pvTz and 6-311G basis sets are capable of producing reasonably good molecular orbital binding energies and kinetic energies. Although the aug-cc-pvTz basis set is larger than 6-311G, it is well known that this basis set works well in optimizing the electron-electron correlation energy. However, in BEB-based calculations, the first ionization potential is taken from experimental data, and the correlation ener-

gies for the subvalence orbitals of these molecules shown in Fig. 1 are not important. Therefore, the GBEB (aug-cc-pvTz) and the GBEB (6-311G) results are in close agreement with each other in spite of the different basis sets employed to model the binding energies. The GBEB cross sections lie between the BEB ($u/3$) and the BEB (6-311G) results at low-incident energies and are slightly larger than these two BEB estimations at high-incident energies. The BEB ($u/3$) model produces the largest cross sections at low-incident energies (sometimes overestimating the experimental data) due to the use of reduced kinetic energies for molecular orbitals with the lowest binding energies, while the BEB (6-311G) predictions produce the smallest cross sections throughout the incident energy range because it overestimates the acceleration energies of the incident electrons. All these models tend to overlap at high-incident energies. Among these cross sections, the GBEB predictions (without any *ad hoc* correction) are in better agreement with the experimental data than the the BEB ($u/3$) and BEB (6-311G).

B. Triatomic molecules

Figure 2 compares the present GBEB (aug-cc-pvTz) and GBEB (6-311G) ionization cross sections of the triatomic molecules H_2O , SO_2 , and CS_2 with the BEB (6-311G) and BEB ($u/3$) results by Hwang *et al.* [27] and Kim *et al.* [29]. For the CS_2 molecule, another two existing BEB calculations (BEB-AE and BEB-ECP) of Scott and Irikura [34] with corrections (i) and (ii), respectively, are also shown. Unlike other models, these two models include scaling parameters that were chosen explicitly to minimize the root-mean-square difference with respect to the experimental data by Rao *et al.* [8] and Lindsay *et al.* [17]. In Fig. 2, we also compare the present results with the existing experimental data by Cadez *et al.* [6], Hayes *et al.* [7], Freund *et al.* [15], Rao *et al.* [8], Basner *et al.* [9] (fast beam and mass spectrometer measurements are represented by Basner-fb and Basner-ms, respectively), Tarnovsky *et al.* [10], Lindsay *et al.* [12,17], and Hudson *et al.* [18].

For the H_2O molecule shown in Fig. 2(a), the two overlapped GBEB calculations are in good agreement with the measurements by Bolorizadeh *et al.* [3] especially in the peak region and for incident energies higher than 200 eV. While the original BEB cross sections are generally closer to the experimental data by Straub *et al.* [13]. Both the GBEB and BEB results agrees with the experimental data by Rao *et al.* [16] at low-incident energies below 20 eV. In the medium- and high-energy regions, both GBEB and BEB are smaller than the measurements. In Fig. 2(b), the GBEB (aug-cc-pvTz) cross sections for the SO_2 molecule are within the error bars of the measurements by Basner *et al.* [9] and Lindsay *et al.* [12] for all incident energies. In comparison to the experimental data by Cadez *et al.* [6], our GBEB (aug-cc-pvTz) predictions agree well with their measurements, except for incident energies below 25 eV, while the GBEB (6-311G) results are slightly lower than these measurements for the energies both below 25 eV and above 100 eV. The BEB ($u/3$) results are in good agreement with the experimental data by Basner *et al.* [9], but underestimate the measurements by Cadez *et al.* [6] and Lindsay *et al.* [12] for the high-incident energies. The

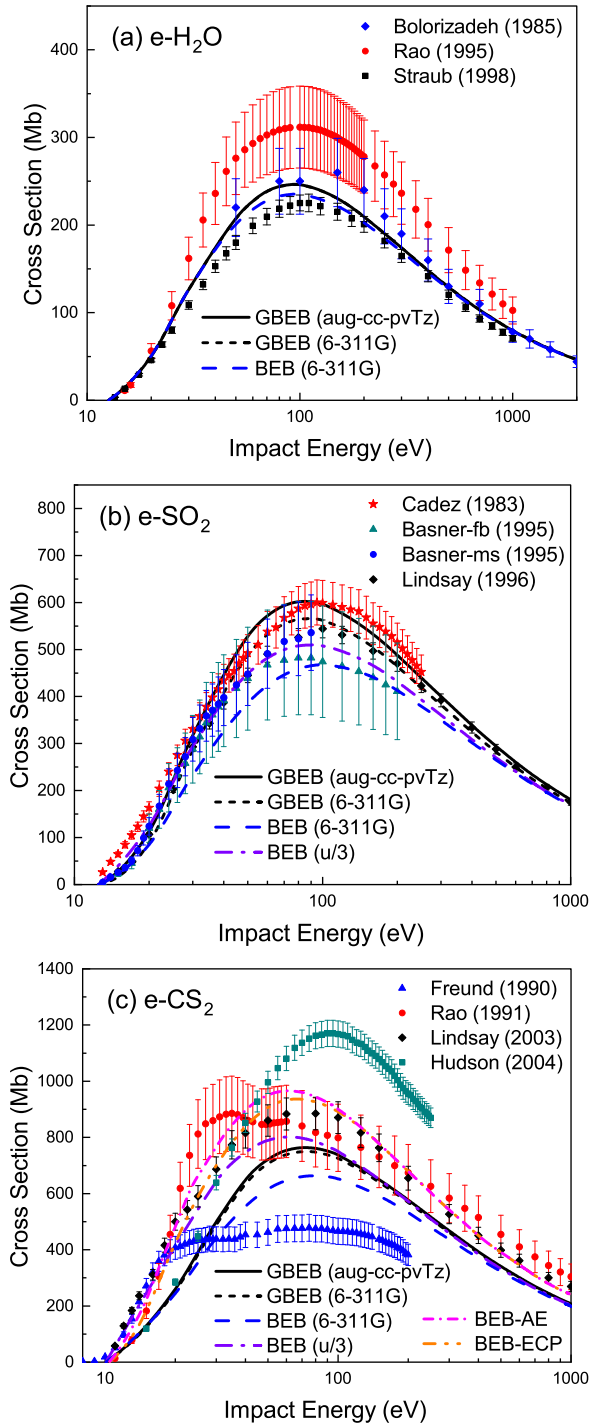


FIG. 2. Total ionization cross sections for triatomic molecules (a) H_2O , (b) SO_2 , and (c) CS_2 . The results of the present GBEB cross sections are shown and compared with the BEB calculations, black solid line: present GBEB (aug-cc-pvTz); black short dashed line: present GBEB (6-311G); blue dashed line: BEB (6-311G) [27,29,30]; purple dashed dotted line: BEB ($u/3$) [27,29,30]; pink short dashed dotted line: BEB-AE [18]; orange dashed dotted dotted line: BEB-ECP [18]. Comparison of the theoretical results with the experimental data are also shown, red stars: Cadez *et al.* [6]; blue diamonds: Bolorizadeh *et al.* [3]; blue triangles: Freund *et al.* [15]; red circles: Rao *et al.* [8,16]; green triangles: Basner-fb *et al.* [9]; blue circles: Basner-ms *et al.* [9]; black diamonds: Lindsay *et al.* [12,17]; green squares: Hudson *et al.* [18].

original BEB model using the 6-311G basis produces results only within the error bars of the fast beam measurements by Basner *et al.* [9]. If considering the experimental errors, the GBEB (aug-cc-pvTz) cross sections show the best predictions. For SO_2 , we notice a significant discrepancy between the GBEB (aug-cc-pvTz) and GBEB (6-311G) results in the region around 100 eV. We attribute these deviations to the large subvalence electron correlation, which can be properly described by the correlation-consistent basis set aug-cc-pvTz.

For the CS_2 molecule, as can be seen in Fig. 2(c), the differences among experimental results are obvious. The present GBEB (aug-cc-pvTz) and GBEB (6-311G) results as well as the BEB ($u/3$) results are in good agreement with the measurements by Rao *et al.* [8] in the incident energy range from about 50 to 250 eV. For low-incident energies, the GBEB predictions and the BEB (6-311G) results agree with the experimental data by Rao *et al.* [8] and Hudson *et al.* [18], while the BEB ($u/3$) results are in agreement with the measurements by Freund *et al.* [15] and Lindsay *et al.* [17]. The scaling parameters of the BEB-AE and BEB-ECP calculations are determined by comparing with experimental data by Rao *et al.* [8] and Lindsay *et al.* [17], which are generally larger than other theoretical results. Therefore, the BEB-AE and BEB-ECP model produced comparably larger cross sections than other theoretical results. The parameter-free GBEB and BEB predictions tend to overlap at high-incident energies because the acceleration corrections affect the cross sections more significantly in relatively low incident energies. The effect of scaling parameters in the BEB ($u/3$) model can be estimated from the comparison with the BEB-AE calculations, which use the similar correction in high-energy range.

As seen from Fig. 2, the differences among theoretical estimations in the total ionization cross sections increase with the complexity of molecules. The slight improvement of the GBEB cross sections compared to the BEB results for the H_2O molecule is only due to the inner core orbital $2a_1$. For simple molecules consisting of atoms with $Z < 10$, the calculation results of GBEB do not differ much from the results of original BEB model which has already successfully predicted the ionization cross sections for simple molecules. The discrepancy between the results of GBEB and BEB become larger if sulfur ($Z = 16$) is included in the molecule. The BEB (6-311G) results are the lowest in magnitude due to the overestimation of the acceleration energies of the incident electrons. The BEB ($u/3$) cross sections are larger in the low-energy range since the employed scaling factor reduces the energies of a few molecular orbitals with small binding energies. Nonetheless, the discrepancy between theoretical calculations and experimental measurements still needs further consideration.

C. Polyatomic molecules

Figure 3 compares the present GBEB (aug-cc-pvTz) and the GBEB (6-311G) calculated ionization cross sections of the polyatomic molecules CH_4 , C_2H_4 , and C_2H_2 with the BEB (6-311G) results by Hwang *et al.* [27] and Kim *et al.* [31]. Due to the improvements in the acceleration correction, GBEB results are generally larger in magnitude than the original BEB calculations. In Fig. 3, we also compare the present results with the existing experimental data by Rapp *et al.* [2], Schram

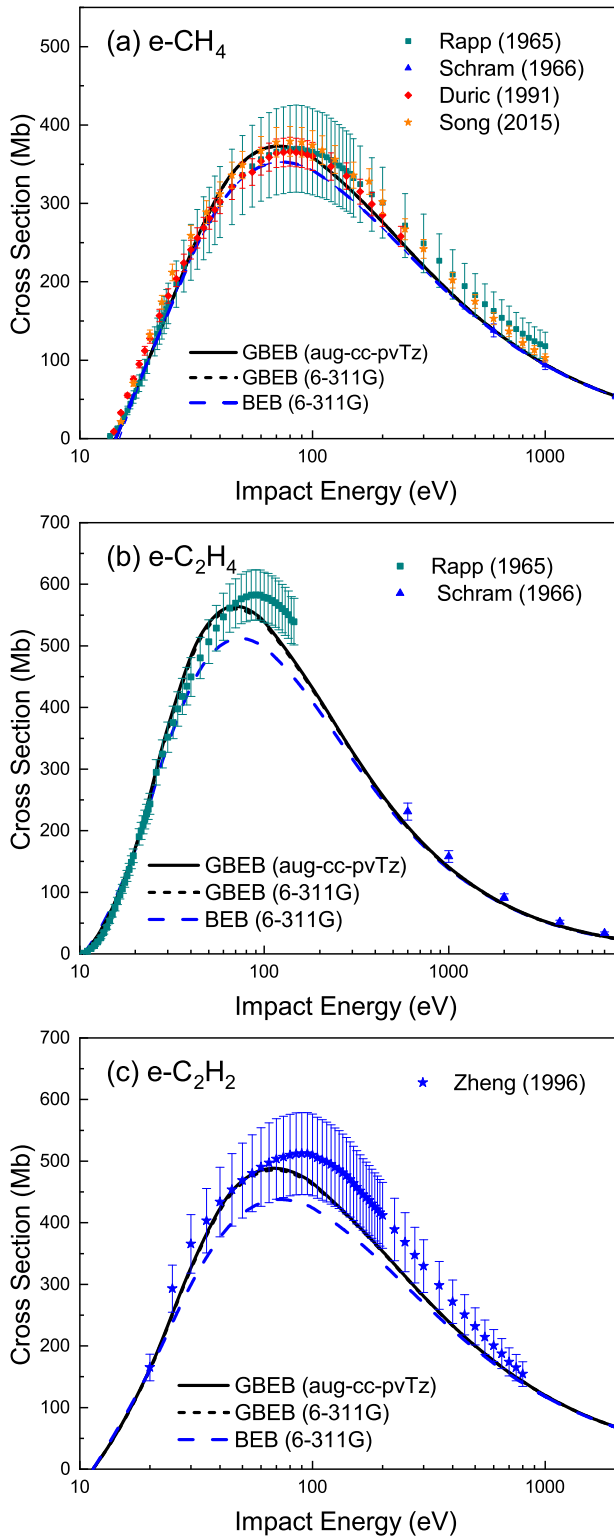


FIG. 3. Total ionization cross sections for polyatomic molecules (a) CH_4 , (b) C_2H_4 , and (c) C_2H_2 . The results of the present GBEB cross sections are shown and compared with the BEB calculations, black solid line: present GBEB (aug-cc-pvTz); black short dashed line: present GBEB (6-311G); blue dashed line: BEB (6-311G) [27,31]. Comparison of the theoretical results with the experimental data are also shown, green squares: Rapp *et al.* [2]; blue triangles: Schram *et al.* [5]; red diamonds: Duric *et al.* [4]; orange stars: Zheng *et al.* [11]; red stars: Song *et al.* [14].

et al. [5], Bolorizadeh *et al.* [3], Duric *et al.* [4], Rao *et al.* [16], Zheng *et al.* [11], Straub *et al.* [13], and Song *et al.* [14].

For the CH_4 molecule shown in Fig. 3(a), two curves of the GBEB (aug-cc-pvTz) and the GBEB (6-311G) cross sections completely merge. This behavior appears because the experimental binding energies are used for the single bonding orbital in both of these two calculations. The GBEB predictions are slightly larger than the BEB (6-311G) estimations due to the improvement of the partial cross sections for core orbital ionization. The GBEB cross sections are generally in better agreement with the existing experimental measurements [2,4,5,14] than the BEB (6-311G) results. The BEB (6-311G) results are lower than the GBEB predictions because they overestimate the kinetic energies gained by the incident electron for core orbital ionization. In Fig. 3(b), the GBEB (aug-cc-pvTz) results are slightly higher than the GBEB (6-311G) calculations due to the relatively large correlation energies for the sub-valence orbitals in the C_2H_4 molecule. The GBEB cross sections are within the error bars of the measurements by Schram *et al.* [5] and in better agreement with experimental data than the BEB calculations by Kim *et al.* [31]. In Fig. 3(c), the GBEB cross sections for the C_2H_2 molecule also show better agreement with the experimental data by Rapp *et al.* [2] than the original BEB cross sections by Hwang *et al.* [27], especially in the peak value. For large incident energies, all theoretical results slightly underestimate the experimental data by Zheng *et al.* [11].

Through the comparison of theoretical results, for the CH_4 molecule the two curves of the GBEB cross sections completely merge, and for the C_2H_4 and C_2H_2 molecules the differences between the GBEB (aug-cc-pvTz) and the GBEB (6-311G) are not obvious because the correlation effect in the subvalence orbital is weak. The discrepancy between the GBEB and BEB predictions is small for the CH_4 molecule. For C_2H_4 and C_2H_2 with double and triple bond valence, respectively, the discrepancies tend to increase.

By increasing the complexity of target molecules, difference between the original BEB results and experimental measurements becomes more pronounced. The difference can be even larger when the component atoms have larger atomic numbers. In the absence of experimental data for the complex molecular targets, the corrections used in previous BEB research are difficult to implement. The present GBEB model will be of great use for practical prediction of the electron impact single ionization cross sections of complex molecules.

IV. CONCLUSION

In this work, we improved the BEB model for the electron-impact ionization cross sections of molecules by incorporating a physically suggested acceleration correction into the molecular orbitals from which the electron is ionized. This correction determined the effective charge seen by the ejected electron. We tested our model on some molecular targets with complexity increasing from diatomic to polyatomic molecules. The calculated total ionization cross sections are in better agreement with the experimental data than those predicted by the original BEB models. The effectiveness of the improved GBEB was thus demonstrated. The total

ionization cross sections of molecules containing atoms with $Z > 10$ could be predicted by the GBEB model without any *ad hoc* corrections. In our future work, we will consider how to obtain the contribution from processes involving intermediate autoionization states to the total ionization cross section.

ACKNOWLEDGMENTS

This work was supported by the National Natural Science Foundation of China (Grant No. 12174147) and the Chinese Scholarship Council (Grants No. 202108210152 and No. 202006175016).

- [1] W. L. Morgan, *Adv. At. Mol. Phys.* **43**, 79 (2000).
- [2] D. Rapp and P. Englander-Golden, *J. Chem. Phys.* **43**, 1464 (1965).
- [3] M. A. Bolorizadeh and M. E. Rudd, *Phys. Rev. A* **33**, 882 (1986).
- [4] N. Duric, I. Cadez, and M. Kurepa, *Int. J. Mass Spectrom. Ion Processes* **108**, R1 (1991).
- [5] B. L. Schram, H. R. Moustafa, J. Schutten, and F. J. D. Heer, *Physica* **32**, 734 (1966).
- [6] I. M. Cadez, V. M. Pejcev, and M. V. Kurepa, *J. Phys. D: Appl. Phys.* **16**, 305 (1983).
- [7] T. R. Hayes, R. C. Wetzel, F. A. Baiocchi, A. Frank, and R. S. Freund, *J. Chem. Phys.* **88**, 823 (1988).
- [8] M. V. V. S. Rao and S. K. Srivastava, *J. Geophys. Res.: Planets* **96**, 17563 (1991).
- [9] R. Basner, M. Schmidt, H. Deutsch, V. Tarnovsky, A. Levin, and K. Becker, *J. Chem. Phys.* **103**, 211 (1995).
- [10] V. Tarnovsky, H. Deutsch, and K. Becker, *J. Chem. Phys.* **105**, 6315 (1996).
- [11] S. H. Zheng and S. K. Srivastava, *J. Phys. B* **29**, 3235 (1996).
- [12] B. G. Lindsay, H. C. Straub, K. A. Smith, and R. F. Stebbings, *J. Geophys. Res.: Planets* **101**, 21151 (1996).
- [13] H. C. Straub, B. G. Lindsay, K. A. Smith, and R. F. Stebbings, *J. Chem. Phys.* **108**, 109 (1998).
- [14] M. Y. Song, J. S. Yoon, H. Cho, Y. Itikawa, G. P. Karwasz, V. Kokoouline, Y. Nakamura, and J. Tennyson, *J. Phys. Chem. Ref. Data* **44**, 023101 (2015).
- [15] R. S. Freund, R. C. Wetzel, and R. J. Shul, *Phys. Rev. A* **41**, 5861 (1990).
- [16] M. V. V. S. Rao, I. Iga, and S. K. Srivastava, *J. Geophys. Res.: Planets* **100**, 26421 (1995).
- [17] B. G. Lindsay, R. Rejoub, and R. F. Stebbings, *J. Chem. Phys.* **118**, 5894 (2003).
- [18] J. E. Hudson, C. Vallance, and P. W. Harland, *J. Phys. B* **37**, 445 (2004).
- [19] S. E. Huber, A. Mauracher, D. Süß, I. Sukuba, J. Urban, D. Borodin, and M. Probst, *J. Chem. Phys.* **150**, 024306 (2019).
- [20] M. C. Zammit, D. V. Fursa, J. S. Savage, and I. Bray, *J. Phys. B* **50**, 123001 (2017).
- [21] L. H. Scarlett, U. S. Rehill, M. C. Zammit, N. A. Mori, I. Bray, and D. V. Fursa, *Phys. Rev. A* **107**, 062804 (2023).
- [22] J. Tennyson, *Phys. Rep.* **491**, 29 (2010).
- [23] R. F. da Costa, M. T. do N. Varella, M. H. F. Bettega, and M. A. P. Lima, *Eur. Phys. J. D* **69**, 159 (2015).
- [24] H. Deutsch, D. Margreiter, and T. D. Märk, *Z. Phys. D* **29**, 31 (1994).
- [25] H. Deutsch, K. Becker, S. Matt, and T. D. Märk, *Int. J. Mass Spectrom.* **197**, 37 (2000).
- [26] Y. K. Kim and M. E. Rudd, *Phys. Rev. A* **50**, 3954 (1994).
- [27] W. Hwang, Y. K. Kim, and M. E. Rudd, *J. Chem. Phys.* **104**, 2956 (1996).
- [28] A. G. Falkowski, M. H. F. Bettega, M. A. P. Lima, and L. G. Ferreira, *Eur. Phys. J. D* **75**, 308 (2021).
- [29] Y. K. Kim, W. Hwang, N. M. Weinberger, M. A. Ali, and M. E. Rudd, *J. Chem. Phys.* **106**, 1026 (1997).
- [30] M. A. Ali, Y. K. Kim, W. Hwang, N. M. Weinberger, and M. E. Rudd, *J. Chem. Phys.* **106**, 9602 (1997).
- [31] Y. K. Kim, M. A. Ali, and M. E. Rudd, *J. Res. Natl. Inst. Stand. Technol.* **102**, 693 (1997).
- [32] H. Nishimura, W. M. Huo, M. A. Ali, and Y. K. Kim, *J. Chem. Phys.* **110**, 3811 (1999).
- [33] W. M. Huo and Y. K. Kim, *Chem. Phys. Lett.* **319**, 576 (2000).
- [34] G. E. Scott and K. K. Irikura, *J. Chem. Theory Comput.* **1**, 1153 (2005).
- [35] G. E. Scott and K. K. Irikura, *Surf. Interface Anal.* **37**, 973 (2005).
- [36] J. N. Bull, M. Bart, C. Vallance, and P. W. Harland, *Phys. Rev. A* **88**, 062710 (2013).
- [37] C. Szmytkowski, P. Mozejko, M. Zawadzki, K. Maciag, and E. Ptasinska-Denga, *Phys. Rev. A* **89**, 052702 (2014).
- [38] W. Y. Baek, M. U. Bug, and H. Rabus, *Phys. Rev. A* **89**, 062716 (2014).
- [39] R. F. da Costa, M. H. F. Bettega, Márcio T. do N. Varella, E. M. de Oliveira, and M. A. P. Lima, *Phys. Rev. A* **90**, 052707 (2014).
- [40] J. Kaur, N. Mason, and B. Antony, *Phys. Rev. A* **92**, 052702 (2015).
- [41] A. K. Arora, V. Sahgal, A. Bharadvaja, and K. L. Baluja, *Phys. Rev. A* **104**, 022816 (2021).
- [42] P. A. S. Randi, G. M. Moreira, and M. H. F. Bettega, *Phys. Rev. A* **107**, 012806 (2023).
- [43] D. Gupta, H. Choi, S. Singh, P. Modak, B. Antony, D. C. Kwon, M. Y. Song, and J. S. Yoon, *J. Chem. Phys.* **150**, 064313 (2019).
- [44] V. Graves, B. Cooper, and J. Tennyson, *J. Chem. Phys.* **154**, 114104 (2021).
- [45] Y. C. Wang, L. Jiao, and S. Fritzsche (unpublished).
- [46] C. C. Montanari and J. E. Miraglia, *J. Phys. B* **47**, 105203 (2014).
- [47] Y. K. Kim, J. P. Santos, and F. Parente, *Phys. Rev. A* **62**, 052710 (2000).
- [48] K. Fedus and G. P. Karwasz, *Phys. Rev. A* **100**, 062702 (2019).
- [49] R. Rejoub, B. G. Lindsay, and R. F. Stebbings, *Phys. Rev. A* **65**, 042713 (2002).
- [50] Q. Sun, T. C. Berkelbach, N. S. Blunt, G. H. Booth, S. Guo, Z. Li, J. Liu, J. McClain, E. R. Sayfutyarova, S. Sharma, S. Wouters, and G. Chan, *Wiley Interdiscip. Rev.: Comput. Mol. Sci.* **8**, e1340 (2017).
- [51] DIRAC, a relativistic *ab initio* electronic structure program, Release DIRAC23 (2023), written by R. Bast, A. S. P. Gomes, T. Saue and L. Visscher, and H. J. Aa. Jensen, with contributions from I. A. Aucar, V. Bakken, C. Chibueze, J. Creutzberg, K. G. Dyall, S. Dubillard, U. Ekström, E. Eliav, T. Enevoldsen,

- E. Faßhauer, T. Fleig, O. Fossgaard, L. Halbert, E. D. Hedegård, T. Helgaker, B. Helmich-Paris, J. Henriksson, M. van Horn, M. Iliáš, Ch. R. Jacob, S. Knecht, S. Komorovský, O. Kullie, J. K. Lærdahl, C. V. Larsen, Y. S. Lee, N. H. List, H. S. Nataraj, M. K. Nayak, P. Norman, A. Nyvang, G. Olejniczak, J. Olsen, J. M. H. Olsen, A. Papadopoulos, Y. C. Park, J. K. Pedersen, M. Pernpointner, J. V. Pototschnig, R. di Remigio, M. Repisky, K. Ruud, P. Sařek, B. Schimmelpfennig, B. Senjean, A. Shee, J. Sikkema, A. Sunaga, A. J. Thorvaldsen, J. Thyssen, J. van Stralen, M. L. Vidal, S. Villaume, O. Visser, T. Winther, S. Yamamoto, and X. Yuan (available at <https://doi.org/10.5281/zenodo.7670749>, see also <https://www.diracprogram.org>).
- [52] S. G. Lias, J. F. Liebman, R. D. Levin, and S. A. Kafafi, NIST Positive Ion Energetics Database, Version 2.0, Standard Reference Database 19A, National Institute of Standards and Technology, 1993.